Protein Nanoparticles Formation by Supercritical Antisolvent with Enhanced Mass Transfer

Pratibhash Chattopadhyay and Ram B. Gupta
Dept. of Chemical Engineering, Auburn University, Auburn, AL 36839

In recent years, the supercritical antisolvent (SAS) precipitation technique has emerged as a promising method for the formation of fine particles. Despite its numerous advantages, this technique still cannot be used to produce particles in the sub-micron range (< 300 nm) for many "soft" materials. A significantly improved SAS process can produce particles of controllable size, up to an order of magnitude smaller than those of the conventional SAS process, with a narrower size distribution. Like the conventional SAS technique, this new supercritical antisolvent with enhanced mass transfer technique utilizes supercritical carbon dioxide as the antisolvent, but the solution jet is deflected by a surface vibrating at an ultrasonic frequency atomizing the jet into much smaller droplets. Furthermore, the ultrasound field generated by the vibrating surface enhances mass transfer and prevents agglomeration through increased mixing. The particle size is controlled by varying the vibration intensity of the deflecting surface, which then can be adjusted by changing the power supplied to the attached ultrasound transducer. It is demonstrated by the formation of lysozyme nanoparticles and microparticles. The biological activity of the protein is retained during the processing.

Introduction

The application of supercritical fluids in the area of materials processing offers considerable promise as a means for the production of particulate biological materials, such as proteins, for use in advanced drug delivery systems. New particle technologies based on SAS precipitation provide protein particles with sizes ranging from 1–10 μm (Yeo et al., 1993; Winters et al., 1996). The major merits of these processes include: production of organic-solvent free particles, mild operating temperatures for processing biological materials, and easier micro-encapsulation of drugs for controlled release of the therapeutic agents. Unfortunately, none of these techniques can produce small protein particles in the sub-micron range (< 300 nm) having a very narrow size distribution. Interesting properties of the particles might be observed at smaller sizes, and it is therefore important to explore possible improvements that can be employed in the current methods for producing nanoparticles (Siegel, 1993).

In recent years, new and complex drugs such as proteins and peptides have become readily available through genetic engineering. The delivery of these drugs is often more complicated than that of other conventional drugs (Langer, 1990). Controlled release systems for these drugs are possible through formulations that consist of protein particles encapsulated within a polymer matrix. An important factor affecting the release rate of these encapsulated protein particles is particle size. The smaller the particles, the higher the percentage of solids that can be incorporated. Also, the particle distribution can be more uniform within the composite structure. Further, submicron size particles are better at dissolving in the blood stream and reaching desired target organs like the heart and the lung tissues (Kreuter, 1983; Gesler et al., 1973; Schroeder et al., 1978).

Conventional technologies, for example, spray drying (Nass, 1988) and milling (Hixon et al., 1990; Van Cleef, 1991) produce particles ranging from 5–50 μm, but protein particles manufactured by these processes usually tend to be denatured. Fluid energy grinding can produce particles in the range of 1–10 μm, but it involves the use of high velocity compressed air, which leads to electrostatically charged powders. Lyophilization (Briggs and Maxwell, 1975) is another technique for protein particle formation, but not all proteins can be lyophilized into stable products, and, besides, the process needs to be tailored to each individual protein. Hence, a number of challenges and problems exist with these conventional methods of particle formation that need addressing.

Correspondence concerning this article should be addressed to R. B. Gupta.

Supercritical fluid technologies such as Rapid Expansion of Supercritical Solutions (RESS) and SAS are fast emerging as efficient, clean, and economically viable methods for biological particle processing. The particles obtained by these processes are 1–5 μm in size and have a narrow size distribution (Chattopadhyay and Gupta, 2000; Turk, 1999) Several researchers have utilized the properties of supercritical CO_2 to develop small particles of various protein and drug molecules. Chang and Randolph (1989) used the RESS technique to produce beta-carotene particles having a narrow size distribution. Larson and King (1985) showed that it is possible to precipitate various steroid particles using supercritical fluids. Later, Steckel et al. (1997) micronized different steroid particles for pulmonary delivery using supercritical fluids. Yeo et al. (1993) used the SAS technique to produce biologically active insulin powder. Sloan et al. (1998) used supercritical fluids and a coaxial tube arrangement to produce biologically active lysozyme particles. Winters et al. (1996) used the SAS technique to generate biologically active micron size particles of lysozyme, trypsin, and insulin. Although these techniques are becoming increasingly popular because of numerous advantages, further developments are necessary to provide a better size control, in order to generate smaller particles having a narrower size distribution.

A significant improvement in the SAS process is presented in this work. The new process, supercritical antisolvent with enhanced mass transfer (SAS-EM), uses a surface vibrating at an ultrasonic frequency to atomize the jet into microdroplets (Gupta and Chattopadhyay, 2000). The ultrasound field generated by the vibrating surface enhances turbulence and mixing within the supercritical phase, resulting in a high mass transfer between the solution and the antisolvent. The combined effect of fast rate of mixing between the antisolvent and the solution, and reduction of solution droplet size due to atomization, provides particles up to ten-fold smaller than those obtained from the conventional SAS process. Figure 1 and Table 1 illustrate the broad differences between SAS-EM and the SAS processes.

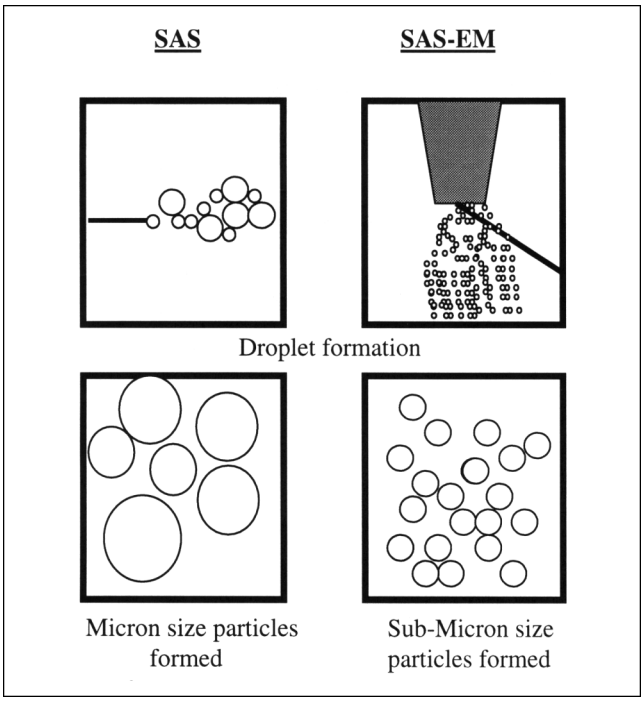

Figure 1. Broad differences between the SAS (Left) and SAS-EM (Right) techniques, respectively.

The objective of this article is to report the features of SAS-EM technique in particle processing and to demonstrate it by the formation of lysozyme nanoparticles for pharmaceutical purposes. Process parameters for the control of particle size are also studied.

Experimental Studies

Materials

All the materials were used as received: CO_2 and N_2 (99.9% pure, Airco), lysozyme (Sigma lot no. 57H7045), bacteria *micrococcus lysodeikticus* (Sigma lot no. 39H8615), dimethylsulfoxide (DMSO, Fisher Scientific), NaCl (99.9% pure, Fisher Scientific), and phosphate buffer (pH = 7, Fisher Scientific).

Apparatus

The apparatus is shown in Figure 2. The apparatus provides for visual observation of phase behavior, precipitation,

Table 1. Differences Between the Conventional SAS Technique and the New SAS-EM Technique

SAS Technique	SAS-EM Technique
Droplet formation	
Droplet formation is due to jet breakup of the solution jet injected into the supercritical fluid phase medium.	Droplet formation is due to atomization of the jet into micro-droplets caused by the horn surface vibrating at an ultrasonic frequency of 20 KHz.
Mass-transfer rate	
Depends on the solvent in use and is the rate of transfer between the droplet and the SCF medium.	Also depends on the solvent in use, but there is an enhanced rate of mass transfer between the droplet and the supercritical fluid due to increased mixing and turbulence caused by the ultrasonic field.
Droplet/particle motion	
Droplet/particle motion within the supercritical fluid phase is due to the momentum imparted by the solution jet velocity.	Droplet/particle motion within the supercritical fluid phase is due to the vibrating ultrasonic surface, which propels the droplets away from the horn surface at a rapid rate.
Particle sizes obtained	
Sizes of the particles obtained are fairly small, in the micrometer range (1–5 μm).	Sizes of the particles obtained are much smaller in the nanometer range (100–500 nm).
Particle–size adjustability	
Particle sizes can be slightly controlled by changing the density of the supercritical fluid, which, in turn, can be changed by varying the pressure and the temperature of the supercritical fluid.	Particle sizes can be controlled to a great extent by changing the power supplied to the vibrating surface (that is, by changing the amplitude of the vibrating surface). In addition, a minor control of particle size may also be obtained by changing the supercritical fluid density.

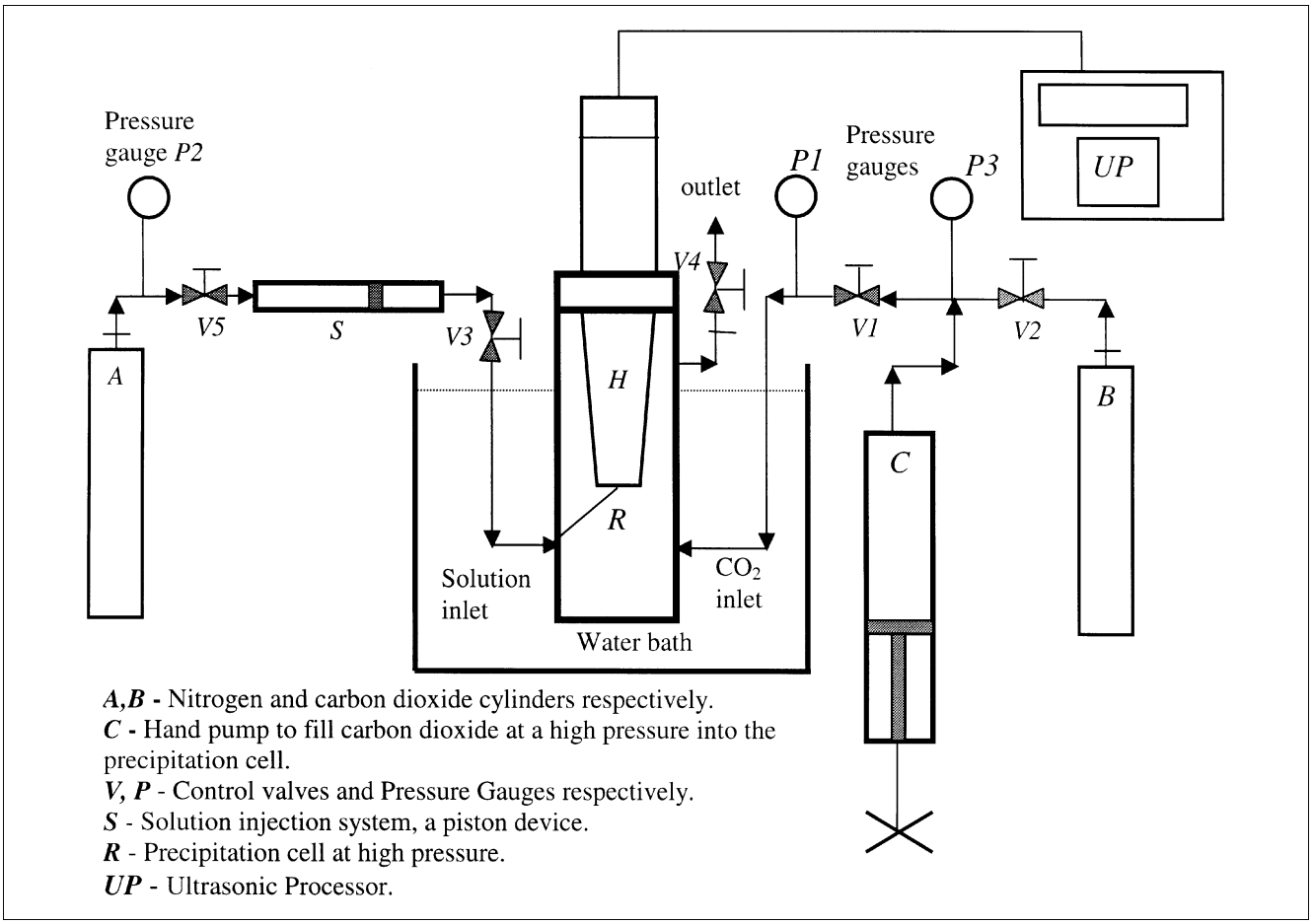

Figure 2. Apparatus for particle production using the SAS-EM technique.

rapid equilibration, and collection of the precipitated particles. The central feature of the apparatus consists of a high-pressure ultrasound precipitation cell (R) approximately 80 cm^3 in volume. A titanium horn (Sonics and Materials) having a broad tip (1.25 cm in diameter) is attached to the precipitation cell for jet deflection and introduction of the ultrasonic field. The ultrasound horn is powered by a 600 W, 20 ± 0.05 kHz ultrasonic processor (Ace Glass, Inc.). The amplitude of vibration of the horn surface is directly proportional to the input power and can be directly controlled by adjusting the power supplied to the ultrasound transducer. A collection plate is placed inside the precipitation cell for collecting the particles. High pressure inside the cell is generated using a HIP hand pump (C). Valves $V1$ and $V2$ are used to fill up the HIP hand pump with fresh CO_2. The entire cell assembly is maintained at a constant temperature using a circulating water bath. The lysozyme solution is injected inside the precipitation cell using a "solution injection device" (S), which consists of a stainless steel cylinder containing a piston. The piston divides the cylinder into two chambers. The protein solution is placed inside one of these chambers and then delivered into the cell by using pressurized nitrogen in the other chamber. The device S is connected to the precipitation cells by means of a 75-μm (internal diameter) fused quartz capillary tube. The capillary tube opening is placed at an angle of about 40° touching the horn surface. Supercritical CO_2 is fed inside the precipitation cell through the inlet port located at the bottom of the vessel. Valve $V1$ is used to control the flow of supercritical CO_2 into the cell. Pressure inside the cell is measured using a pressure gauge $P1$. The outlet port is located on top of the precipitation cell and valve $V4$ is used to control the depressurization process. The pressure difference across the capillary is measured using the pressure gauges $P2$ and $P1$.

Procedure

All the precipitation experiments were carried out in batch mode. The first step was filling up the precipitation cell with carbon dioxide to obtain the desired pressure. The temperature inside the chamber was maintained constant by placing it in a water bath. Lysozyme solution in DMSO (concentration, 5 mg/mL) was loaded into the "solution injection device." The titanium horn (H) inside the precipitation cell was then allowed to vibrate at the desired amplitude by adjusting the input power, and the lysozyme solution was introduced inside the precipitation chamber through the 75 μm capillary tube, placed against the horn surface. As soon as the solution jet was in contact with the vibrating horn surface, it was atomized into tiny droplets and lysozyme particles were formed due to the rapid removal of DMSO by supercritical CO_2 from these droplets. The mass-transfer rate between DMSO and

supercritical CO_2 was greatly enhanced due to increased mixing caused by the ultrasonic field generated by the horn surface. Increased mixing also led to an increase in particle motion inside the precipitation cell, and this prevented agglomeration.

Next was the cleaning step in which DMSO that was left dissolved in supercritical CO_2 was removed by continuously purging with fresh CO_2. The complete cleaning process required approximately 7–8 times the vessel volume of fresh CO_2. The precipitation cell was then allowed to slowly depressurize until it reached ambient pressure. The chamber was then opened and the collection plate was removed and taken for particle analysis.

Particle-size analysis

Analysis was carried out using Scanning electron microscopy (Zeiss, model DSM940). The samples were coated with gold/palladium using a sputter coater (Pelco, model Sc-7). From the SEM micrographs, both the volume-based and the number-based size distributions were determined by measuring the diameters of about 100–200 randomly selected particles for each experiment.

Results

The ultrasonic processor is designed to deliver a constant amplitude. The amplitude of vibration of the ultrasound horn surface can be controlled by adjusting the total power it delivers. The higher the power supplied to the ultrasonic transducer, the greater are the vibrations at the horn tip and the higher is the horn amplitude. As the load or pressure on the horn face increases, the power supply automatically boosts up to ensure that the amplitude remains as selected.

The solution jet atomization and mixing within supercritical media are closely related to the degree of vibrations of the horn surface and, hence, interesting behavior of the precipitation process can be observed at different horn amplitudes. Experiments were conducted to examine the effect of change in the horn amplitude on the size of the lysozyme particles formed. The precipitation cell was kept constant at 96.5 bar and 37°C, and the frequency of the ultrasound horn was maintained at 20 kHz. The solution jet was introduced into the cell at different horn amplitudes corresponding to 0–20% of the total output power (600 W). Different lysozyme particle sizes were obtained from each of these experiments, as listed in Table 2. Figures 3a–3f are SEM micrographs of particles obtained from experiments conducted at the different horn amplitudes. Figures 4a–4f show a comparison of particle-size distribution of lysozyme particles obtained in each of these experiments. Figure 5 is an SEM image of the untreated lysozyme sample as obtained from the manufacturer. A comparison of Figures 3a–3f and Figure 5 clearly illustrate the differences in morphology and sizes of particles obtained after the precipitation process.

Table 2. Experiments Conducted at Different Values of Ultrasound Power Supply at 96.5 bar and 37°C

Power Supplied (W)	SIze Num. Avg. (nm)	Size Vol. Avg. (nm)	Std. Dev. (nm)
0	1,200	2,000	640
12	730	1,040	490
30	650	860	410
60	240	260	75
90	190	190	180
120	230	360	160

Ultrasound Horn Amplitude (or Ultrasound Power) as a Size Tuning Parameter

The above results show that, without ultrasound (that is, when the ultrasound horn amplitude is zero), the volumetric mean size of particles was 2 μm with a standard deviation of 1 μm. The experiment conducted at zero amplitude was basically the conventional SAS technique, and the nozzle in this case was kept parallel to the horn surface. Similar results have been obtained by Winters et al. (1996) in their SAS experiments. The lysozyme particle sizes obtained by them were around 1–5 μm. Experiments conducted at higher amplitudes yielded a considerable decrease in particle size to as low as 190 nm in case of horn amplitude corresponding to a 90 W power supply (Table 2). Figure 6 shows the relationship between average particle size and the ultrasound power corresponding to different amplitudes. The volumetric average (S_{vol}) and number average (S_{num}) particle sizes at different ultrasound power (P) decreases with increasing power as

$$S_{vol} = 0.211P^2 - 39.791P + 1744.8 \quad (1)$$

$$S_{num} = 0.115\,7P^2 - 21.097P + 1113.7 \quad (2)$$

where S_{vol} and S_{num} are in nm and P is in Watts.

From Figure 6, one can infer that the mean particle size decreases to a minimum at the horn amplitude corresponding to a 90 W power supply. Increasing the amplitude beyond this point tends to increase particle size by a small amount. This may be due to the detrimental effects of very high mixing that can increase agglomeration. Apart from a decrease in the particle size, there is also a considerable decrease in the standard deviation of particles at higher probe amplitudes, as shown in Figure 7. This may be due to the narrow droplet-size distribution obtained in the SAS-EM technique, which leads to the formation of more uniformly sized particles.

Bindal et al. (1986) studied the variation in droplet-size distribution as a function of amplitude variation for atomizers with the liquid flowing through a channel within the ultrasonic horn. They observed that there is an increase in the droplet size with increase in amplitude and which was attributed to cavitation in the liquid flowing through the channel even before it comes out on to the surface. In our case, due to high operating pressure (96.5 bar) and also since the liquid hits against the horn surface as opposed to traveling through a channel in the horn, cavitation effects are absent.

Discussion

Volumetric expansion of DMSO

The working of the antisolvent precipitation technique is closely related to the volumetric expansion of the carrier solvent when in contact with the supercritical fluid (SCF) anti-

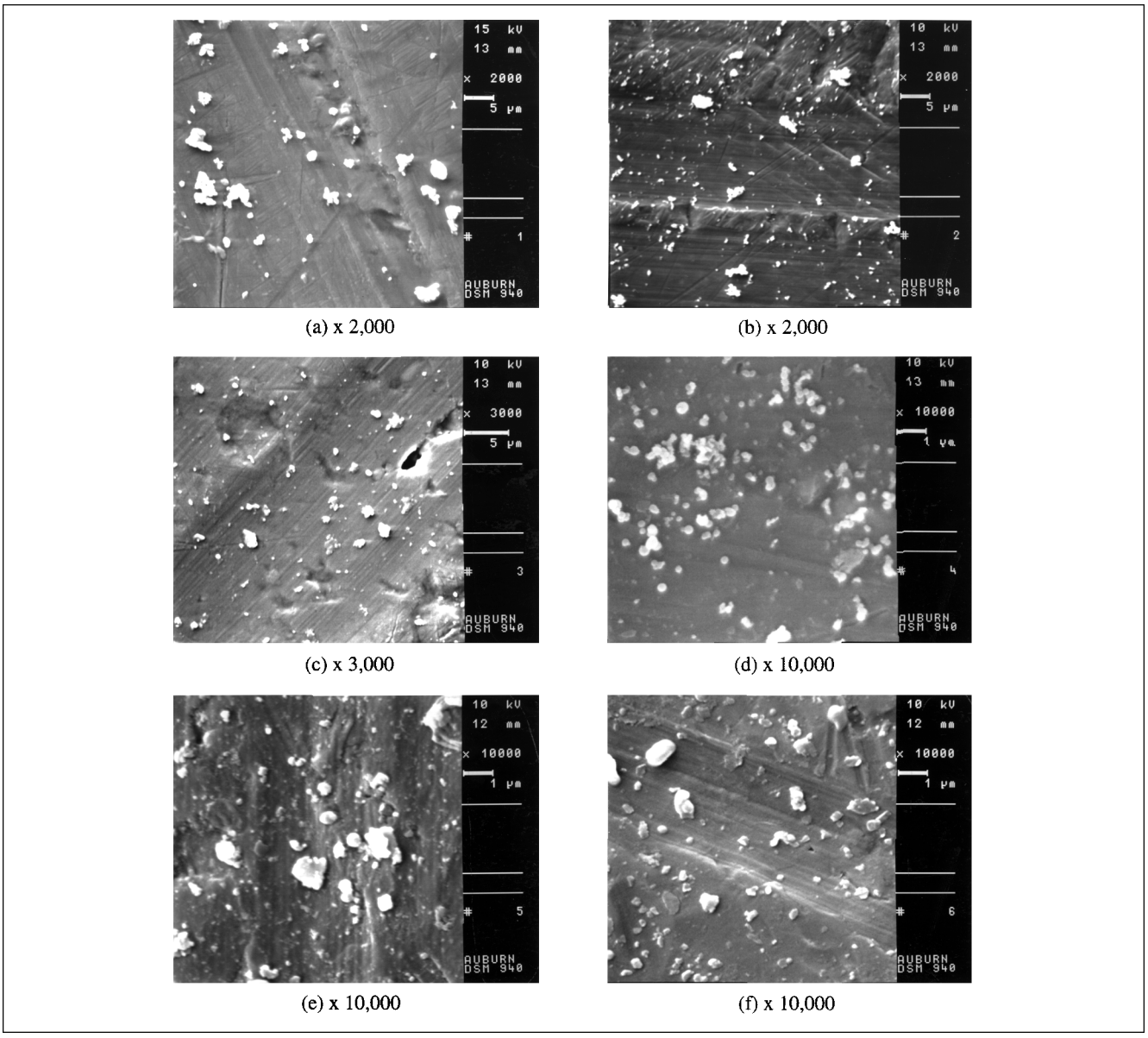

Figure 3. SEM micrographs of the particles obtained from experiments at different ultrasound powers.

(a) 0 W, (b) 12 W, (c) 30 W, (d) 60 W, (e) 90 W, and (f) 120 W. The volume-average particle sizes are: (a) 2,000 nm, (b) 730 nm, (c) 653 nm, (d) 240 nm, (e) 189 nm, and (f) 227 nm.

solvent. The volumetric expansion behavior for the DMSO-CO_2 system has been reported by Yeo et al. (1993) at temperatures of 22 and 35°C. Volumetric expansion of DMSO with supercritical CO_2 has also been calculated by Korkikowski et al. (1995) for 25 and 30°C and by Reverchon et al. (1998) between the temperature range of 35–70°C. All these results clearly illustrate that CO_2 produces a remarkably high volumetric expansion of DMSO, reaching as high as 1,000% near the mixture's critical point.

Deflection effect of the vibrating surface

When a solution is sprayed onto the horn surface, the liquid spreads evenly over the surface forming a thin liquid film. Since the horn surface is vibrating at a fixed frequency of 20 kHz, a set of waves appears on the free liquid surface. The oscillatory vibrations of the fluid surface cause the waves to increase in amplitude until the tips break off and droplets are emitted from the surface into the media (Lang, 1962), as illustrated in Figure 8.

The droplet diameter is proportional to the wavelength of the liquid surface waves, and can be determined by the following relation (Topp, 1973)

$$D = 0.34\left(\frac{8\pi\sigma}{\rho f^2}\right)^{1/3} \tag{3}$$

where σ is the surface tension, ρ is the density of the liquid, and f is the working frequency. Later, Sindayihebura et al.

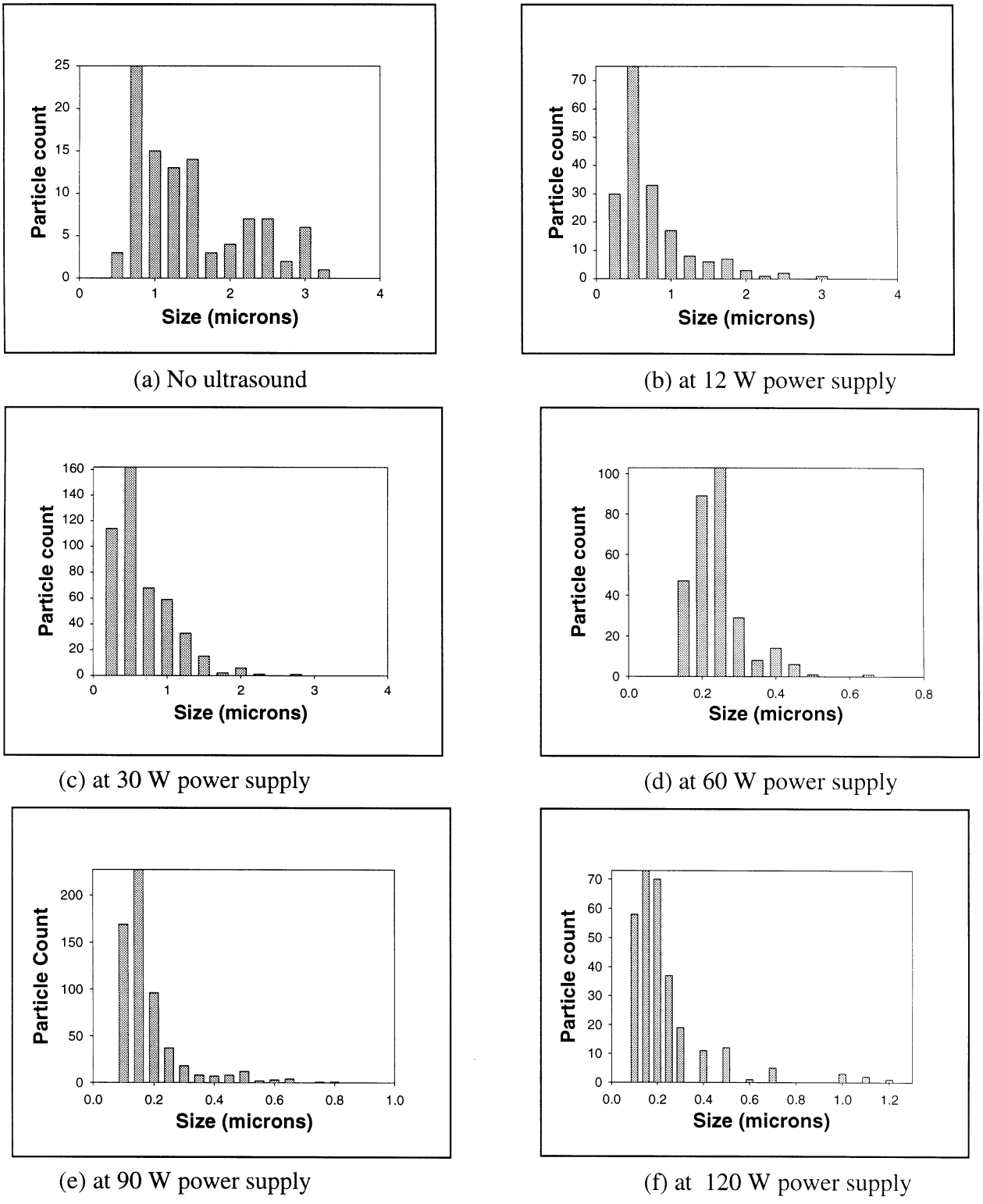

Figure 4. Particle-size distribution of lysozyme particles obtained from experiments conducted at different ultrasound power.

(1997) suggested a linear relationship relating droplet diameter and the surface wavelength as

$$D = K\lambda_s \tag{4}$$

where D is the mean droplet diameter, K is a constant determined from droplet-size distribution, and λ_s is the surface wavelength obtained from stability analysis of the free liquid surface on the horn using continuity and Navier-Stokes equa-

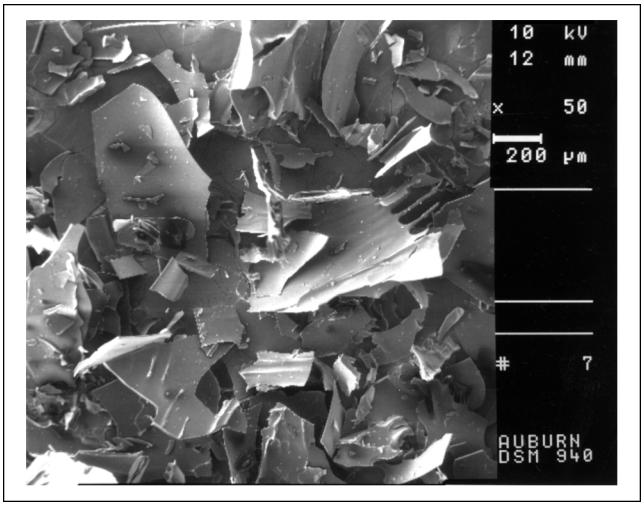

Figure 5. SEM micrograph of untreated lysozyme sample as obtained from the manufacturer.

tions (Sindayihebura et al., 1997)

$$\frac{2}{\pi f^2 \lambda_s}\left(\frac{4\sigma\pi^2}{\rho\lambda_s^2}+g\right)\tanh\left(\frac{2\pi h}{\lambda_s}\right)+0.2\left[\frac{\pi\alpha_o}{\lambda^s}\tanh\left(\frac{2\pi h}{\lambda_s}\right)\right]^{1/2}-1.04=0 \quad (5)$$

where f is the working frequency, α_o is the amplitude of the atomizing surface, g is the acceleration due to gravity, σ is the surface tension, ρ is the supercritical fluid density, and h is the thickness of the liquid on the horn surface.

Once the droplets are present inside the supercritical fluid, rapid transfer of CO_2 into these droplets and DMSO out of these droplets causes the droplets to expand rapidly, which subsequently decreases the droplet's ability to keep the lysozyme molecules dissolved, causing the lysozyme to precipitate as fine particles. The precipitation starts at the supercritical fluid-liquid interface and then propagates inside the liquid droplet attracting the solute towards the interface (Bertucco et al., 1997), which causes the formation of the porous spherical balloon like structures made up of tiny lysozyme particles loosely coalesced together. Such spherical structures up to 20 μm in diameter were observed by Reverchon et al. (1998) and Reverchon (1999) in case of AcY particles using DMSO as the solvent. Similar structures have also been observed in our case for experiments conducted at 96.5 bar, 37°C, and a small ultrasound horn amplitude corresponding to 0–2% of the total power supply. In our case the sizes of these structures are a lot smaller and range between 1–5 μm, as shown in Figure 9. This decrease in the size may be due to smaller initial droplet diameter and narrower droplet-size distribution produced by the SAS-EM technique when compared to the conventional SAS technique. These structures, however, are not seen at higher amplitudes since increased ultrasonic waves can break the balloon like structures into their individual particles.

Another important factor that influences the protein particle size is the mass-transfer rate of the supercritical fluid into

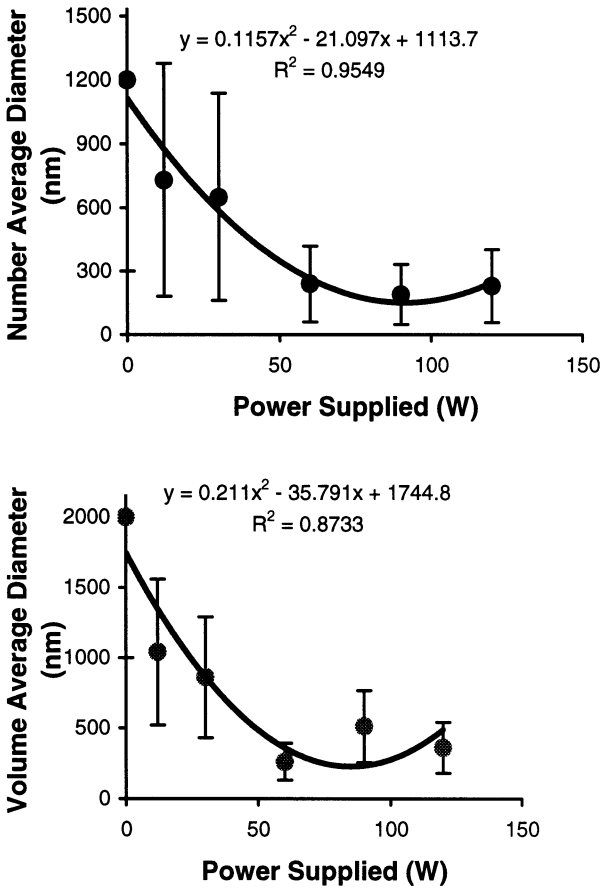

Figure 6. Mean lysozyme particle size vs. power supply to the horn.

the liquid droplet. Mass transfer between supercritical CO_2 and DMSO causes the lysozyme particles to precipitate out as tiny nuclei, which in turn coalesce together forming larger protein particles. Better mixing characteristics can thus affect particle size by enhancing mass-transfer rates between the solution and the supercritical phase and also by preventing the particle from agglomerating together (Palakodaty and

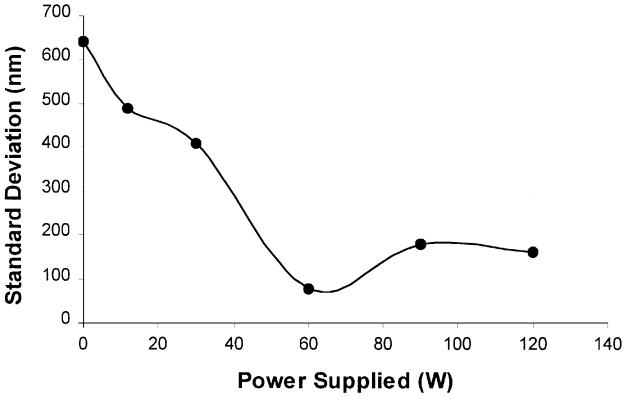

Figure 7. Standard deviation of lysozyme particle size vs. power supply to the horn.

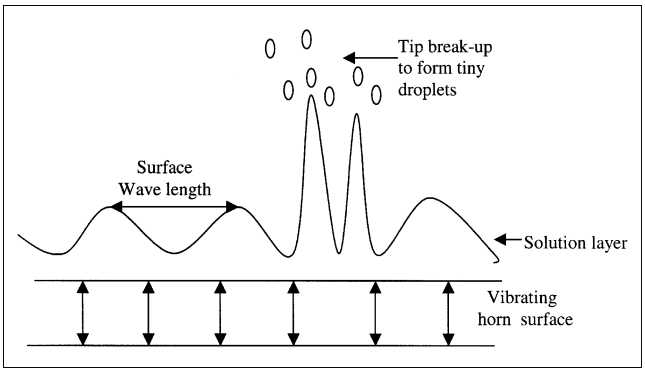

Figure 8. Disintegration mechanism of the liquid film on the horn surface (Drews et al., 1979).

York, 1999). Furthermore, Randolph et al. (1993) have shown that mass-transfer rates are more important than the initial droplet size in determining particle size.

Several researchers (Mandralis and Feke, 1993; Apfel, 1990; Schram, 1988) have demonstrated that ultrasonic standing waves at appropriate intensities can cause increased particle motion due to the nonuniform distribution of pressure and velocity components in the standing ultrasonic wave field. This same phenomenon is observed in the SAS-EM technique. The ultrasound field generated inside the precipitation chamber greatly enhances turbulence within the supercritical phase resulting in a high mass transfer due to increased mixing and also prevents agglomeration of particles. In the SAS-EM technique, the combined effects of jet atomization into very tiny droplets and high rates of mass transfer due to increased mixing within the supercritical phase causes the particle sizes to be extremely small.

Lengsfeld et al. (2000) propose that the mechanism of particle formation in the SAS process is due to particle growth in the gaseous plume, and not due to the jet atomization into droplets. Since the surface tension decreases to a negligible value within about 1 μm distance, which is smaller than the characteristic breakup lengths, the jet spreads in a fashion characteristic of a gaseous jet and microparticle formation results due to gas-phase nucleation and growth within the expanding plume, rather than nucleation within discrete liquid droplets. If above theory is correct, then the SAS-EM technique is working by providing a high degree of mixing causing a reduction in the particle growth.

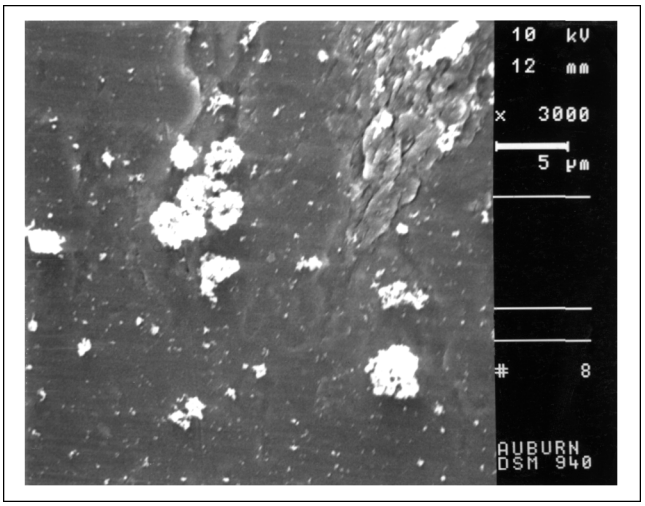

Figure 9. SEM image of lysozyme particles produced by the SAS-EM process at 96.5 bar, 37°C, and 12 W power supply.

In this case the particles are agglomerated together as spherical balloons of sizes ranging from 2–5 μm.

Effect of ultrasound on the lysozyme particles

During the precipitation process, the particles formed remain suspended within the supercritical phase and experience different kinds of gravitational, mechanical, acoustic-radiation-pressure, and hydrodynamic forces. Mechanical forces are exerted on particles when they come in contact with the vibrating horn surface. These forces can be large enough to break the particles into smaller sizes. Acoustic radiation pressures are the differences between the average pressure at a surface moving with the displacement due to the sound and the pressure that would have existed in a fluid of the same mean density at rest (Rayleigh, 1896; King, 1934). The acoustic radiation pressure force drives the particles towards the nodes (or the anti-nodes) of a stationary-sound field. The protein particles suspended in the ultrasonic field oscillate with different velocities and phases relative to one another; as a result, the particles experience a hydrodynamic force known as Bjerknes forces. Bjerknes forces acting between the particles can be attractive and repulsive depending on the phase difference between the velocities of the protein particles (Lamb, 1945). Another type of hydrodynamic force that the particles experience is the Bernoulli's force which arises due to a steady fluid motion around the stationary particles resulting in attraction between them. Bernoulli's forces are responsible for the coagulation of particles at high-frequency ultrasonic fields (Mednikov, 1965).

Apart from displacement forces on protein particles as described above, different types of steady flows also arise in the presence of an ultrasonic field leading to a phenomenon known as ultrasonic streaming. These flows exist both in the ultrasonic free field and near the obstacles. The velocity of these streams can be approximately predicted as (Shutilov, 1988),

$$\rho_o \nu_o^2(x)/2 = w(0) - w(x) \tag{6}$$

where ν_o is the flow velocity, ρ_o is the fluid density, and w is the acoustic energy density. The above equation is the law of conservation of energy where the lefthand side represents the kinetic energy per unit volume of the medium and the right-hand side is the difference between the average acoustic density at the ultrasonic source and at distance x. The flow of liquid inside the chamber is directed away from the ultrasonic radiator and is accompanied by inflow from regions where the liquid encounters a solid obstacle. As a result, continuous stationary circulating currents are generated which keep the particles in constant motion. Depending on the ultrasonic intensity and the size of the vessel, these currents can be laminar or turbulent. At high ultrasonic intensities, the acoustic flow becomes extremely turbulent and gives rise to intense mixing of particles within the fluid.

Effect of ultrasound on the biological activity of lysozyme

As seen in the above results, ultrasound helps favorably in terms of decreasing the particle size. However, for biological molecules, it is also important that no other chemical changes are caused that may reduce the activity of the substance. Since the suspended lysozyme particles are constantly exposed to ultrasound, it is possible that a loss in their activity or denaturization of the protein can occur due to interaction between the ultrasonic field and the particles. In order to examine the effect of ultrasound on the precipitated particles, experiments were conducted to monitor the biological activity of the protein particles exposed to ultrasound in SAS-EM process.

A biological suspension of 20 mg of *micrococcus lysodeikticus* was prepared in 90 mL of phosphate buffer ($pH = 7$) and 10 mL of 1% NaCl solution. Lysozyme solution was prepared in the phosphate buffer having a concentration of 0.04 mg/mL. 0.25 mL of this protein solution was mixed to 2.5 mL of the bacterial suspension. Analysis was carried out by monitoring the rate of absorbance at 450 nm using a UV-Spectrophotometry (Spectronic Genesys 2), as shown in Figure 10. The rate of absorbance was linear for 4 min and was proportional to the concentration of the biological active enzyme. Based on the above results, it follows that lysozyme particles obtained from the SAS-EM technique at an ultrasound horn amplitude corresponding to 60 W power supply, retained about 87% of their activity. The biological activity of the protein is retained during the processing. However, more tests need to be conducted for "labile" proteins to generalize the result.

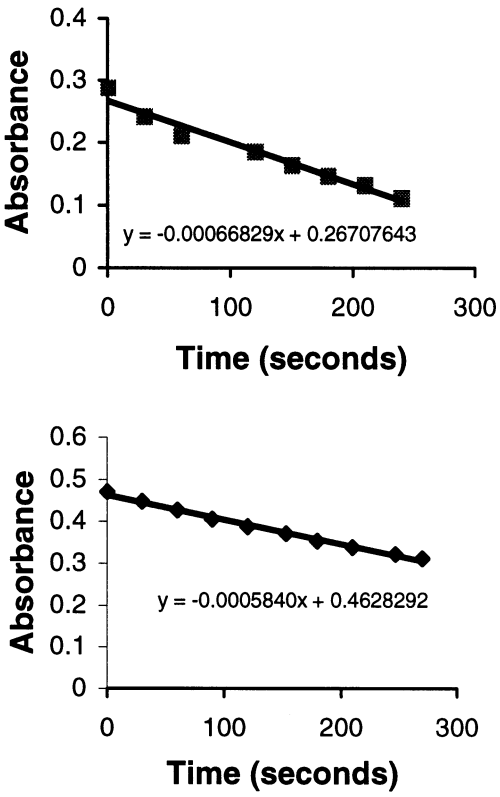

Figure 10. Lysozyme assay tests.

Lysozyme supplied by the manufacturer (top), Lysozyme particles obtained at 96.5 bar, 37°C, and at 60 W ultrasound power supply (bottom). Lysozyme particles obtained by the SAS-EM technique retained about 87% of the original activity.

Conclusions

The SAS-EM technique can be successfully used to produce micro- and nanoparticles of lysozyme. The particles obtained by the new process are up to 10 fold smaller than those obtained from the conventional SAS process. Ultrasound power (that is, horn amplitude) can be used to accurately control the particle size. The particle size decreases with the increase in the ultrasound power up to a certain point beyond which the particle sizes increases slightly. SAS-EM provides a narrower size distribution of particles as compared to the conventional SAS process.

Acknowledgment

Financial support from NSF (CTS-9801067) and NIH (James A. Shannon Director's award to RBG, 1R55RR13398-01) is appreciated. Authors are also thankful to Dr. Lalit Chordia of Thar Designs, Inc. (www.thardesigns.com) for technical discussions.

Literature Cited

Apfel, R. E., "Radiation Pressure—Principles and Application to Separation Science," *Fortschritte der Acustik DAGA*, Wien, **19**, (1990).

Bertucco, A., F. Vaccaro, and P. Pallado, "Drugs Encapsulation Using Compressed Gas Antisolvent Precipitation," *Proc. Italian Conf. on Supercritical Fluids and Their Applications*, Capri, Italy (Sept. 7–10, 1997).

Bindal, V. N., S. K. Jain, and Y. Kumar, "Performance Characteristics of an Ultrasonic Atomizer," *Ind. J. of Technol.*, **24**, 153 (1986).

Briggs, A., and T. Maxwell, "Method of Preparation of Lyophilized Biological Products," U.S. Patent No. 3,928,555 (1975).

Chang, C. J., and A. D. Randolph, "Precipitation of Microsize Organic Particles from Supercritical Fluids," *AIChE J.*, **35**, 1875 (1989).

Chattopadhyay, P., and R. B. Gupta, "Supercritical CO_2-Based Production of Fullerene Nanoparticles," *Ind. Eng. Chem. Res.*, **39**, 2281 (2000).

Drews, W. D., "Flussigkeitszerstaubung durch Ultrascall," *Electronik*, **10**, 83 (1979).

Eckert, C. A., B. L. Knutson, and P. G. Debenedetti, "Supercritical Fluids as Solvents for Chemical and Materials Processing," *Nature*, **383**, 313 (1995).

Gesler, R. M., P. J. Garvin, B. Klamer, R. U. Robinson, C. T. Thomson, W. R. Gibson, F. C. Wheeler, and R. G. Carlson, "The Biological Effects of Polystyrene Latex Particles Administered Intravenously to Rats—a Collaborative Study," *Bull. Parent. Drug Assoc.*, **27**, 101 (1973).

Gupta, R. B., and P. Chattopadhyay, "Method of Forming Nanoparticles and Microparticles of Controllable Size Using Supercritical Fluids and Ultrasound," U.S. Patent Application No. 60/206,644 (2000).

Hixon, L., M. Prior, H. Prem, and J. Van Cleef, "Sizing Materials by Crushing and Grinding," *Chem. Eng.*, **97**, 99 (1990).

King, L. V., "On the Acoustic Radiation on Spheres," *Proc. Roy. Soc. of London*, **A147**, 212 (1934).

Kordikowski, A., A. P. Schenk, R. M. Van Nielen, and C. J. Peters, "Volumetric Expansions and Vapor-Liquid Equilibrium of Binary Mixtures of a Variety of Polar Solvents and Certain Near Critical Solvents," *J. Supercritical Fluids*, **8**, 205 (1995).

Kreuter, J., "Evaluation of Nanoparticles as Drug-Delivery-Systems II: Comparison of the Body Distribution of Micro-Sphere (Diameter > 1 mm), Liposomes, and Emulsions," *Pharm. Acta Helv.*, **58**, 217 (1983).

Lamb, H., "Hydrodynamics," Dover Publications, New York (1945).
Lang, R. J., "Ultrasonic Atomization of Liquids," *J. of Acoust. Soc. of Amer.*, **34**, 6 (1962).
Langer, R. S., "New Methods of Drug Delivery," *Science*, **249**, 1527 (1990).
Larson, F. A., and M. L. King, "Evaluation of Supercritical Fluid Extraction in the Pharmaceutical Industry," *Biotechnol. Prog.*, **2**, 73 (1985).
Lengsfeld, C. S., J. P. Delplanque, V. H. Barocas, and T. W. Randolph, "Mechanism Governing Microparticle Morphology during Precipitation by a Compressed Antisolvent: Atomization vs. Nucleation and Growth," *J. Phys. Chem. B*, **104**, 2725 (2000).
Mandralis, Z. I., and D. L. Feke, "Fractionation of Suspensions Using Synchronized Ultrasonic and Flow Fields," *AIChE J.*, **39**, 197 (1993).
Mednikov, E. P., "Acoustic Coagulation and Settling of Aerosols," Consultants Bureau, New York (1965).
Nass, R., "Pharmaceutical Suspensions," *Pharmaceutical Dosage Forms*, H. A. Lieberman, M. Rieger, and G. Banker, eds., Marcel Dekker, New York, p. 151 (1988).
Palakodaty, S., and P. York, "Phase Behavioral Effects on Particle Formation Process Using Supercritical Fluids," *Pharmaceutical Res.*, **16**, 976 (1999).
Randolph, T. W., A. D. Randolph, M. Mebes, and S. Yeung, "Submicrometer-Sized Biodegradable Particles of Poly(L-Lactic Acid) via the GAS Antisolvent Spray Precipitation Process," *Biotechnol. Prog.*, **9**, 429 (1993).
Rayleigh, B. and J. W. Strutt, *Theory of Sound*, Macmillan, New York (1896).
Reverchon, E., "Supercritical Antisolvent Precipitation of Miro- and Nano-Particles," *J. of Supercritical Fluids*, **15**, 1 (1999).
Reverchon, E., G. Della Porta, A. D. Trolio, and S. Pace, "Supercritical Antisolvent Precipitation of Nanoparticles of Superconductor Precursors," *Ind. Eng. Chem. Res.* **37**, 952 (1998).
Schram, C. J., "Manipulation of Particles," U.S. Patent No. 4,743,351 (1988).
Schroeder, H. G., G. H. Simmons, and P. P. DeLuca, "Distribution of Radiolabelled Subsieve Microspheres after Intravenous Administration to Beagle Dogs," *J. Pharm. Sci.*, **57**, 504 (1978).
Shutilov, V. A., *Fundamental Physics of Ultrasound*, Gordon and Breach Science Publishers, New York (1988).
Siegel, R. W., "Nanostructured Materials," *Adv. Top. Mater. Sci. Eng.*, [Proc. Mex.-U.S.A. Symp.] (1993).
Sindayihebura, D., J. Cousin, and C. Dumouchel, "Experimental and Theoretical Study of Sprays Produced by Ultrasonic Atomizers," *Part. Part. Syst. Charact.*, **14**, 93 (1997).
Sloan, R., G. O. Hollowood, G. O. Humprey, W. Ashraf, and P. York, "Supercritical Fluid Processing: Preparation of Stable Protein Particles," M. Perrut, P. Subra, eds., *Proc. of 5th meeting on Supercritical Fluids*, INPL, Vandeuvre, France, 1 (1998).
Steckel, H., J. Thies, and B. W. Muller, "Micronization of Steroids for Pulmonary Delivery by Supercritical Carbon Dioxide," *Int. J. of Pharm.*, **152**, 99 (1997).
Topp, M. N., "Ultrasonic Atomization—A Photographic Study of the Mechanism of Disintegration," *Aerosol Sci.*, **17**, 17 (1973).
Turk, M., "Formation of Small Organic Particles by RESS: Experimental and Theoretical Investigations," *J. Supercrit. Fluids*, **15**(1), 79 (1999).
Van Cleef, J., "Powder Technology," *Am. Sci.*, **79**, 304 (1991).
Winters, M. A., B. L. Knutson, P. G. Debenedetti, H. G. Sparks, T. M. Przybcien, C. L. Stevenson, and J. S. Prestrelski, "Precipitation of Proteins in Supercritical Carbon Dioxide," *J. of Pharm. Sci.*, **85**, 586 (1996).
Yeo, S.-F., G.-B. Lim, P. G. Debenedetti, and H. Bernstein, "Formation of Microparticulate Protein Powders Using a Supercritical Fluid Antisolvent," *Biotechnol. and Bioeng.*, **41**, 341 (1993).

Manuscript received Jan. 8, 2001, and revision received July 6, 2001.